



Title	Intramolecular hydroamination catalysed by gold nanoparticles deposited on fibrillated cellulose
Author(s)	Uetake, Yuta; Suwattananuruk, Butsaratip; Sakurai, Hidehiro
Citation	Scientific Reports. 2022, 12, p. 20602
Version Type	VoR
URL	https://hdl.handle.net/11094/98573
rights	This article is licensed under a Creative Commons Attribution 4.0 International License.
Note	

The University of Osaka Institutional Knowledge Archive : OUKA

<https://ir.library.osaka-u.ac.jp/>

The University of Osaka



OPEN

Intramolecular hydroamination catalysed by gold nanoparticles deposited on fibrillated cellulose

Yuta Uetake^{1,2}, Butsaratip Suwattananuruk¹ & Hidehiro Sakurai^{1,2}✉

Gold nanoparticles stabilised by fibrillated citric acid-modified cellulose (Au:F-CAC) catalyse the intramolecular cycloamination of amines to unactivated alkenes under an aerobic atmosphere to afford pyrrolidine derivatives. Only 0.2 mol% of Au loading is required to complete the reaction. The high sensitivity of the Au:F-CAC catalyst to the substitution pattern of alkenes allows a unique chemoselective cycloamination, affording new compounds.

The cationic gold complex is one of the most helpful metal catalysts to activate unsaturated bonds, such as alkenes and alkynes (Fig. 1A)^{1–3}. The activated double or triple bonds react with nucleophiles both intermolecularly and intramolecularly to give functional or cyclic compounds^{4,5}. The carbophilic and π -acidic nature of cationic gold species do not lose their electrophilicity in the presence of hard nucleophiles, such as oxygen or nitrogen, allowing the use of nucleophilic reagents, such as amines, hydroxy groups, and water^{6,7}.

In the case of (quasi-)heterogeneous catalysis, gold nanoparticles (Au NPs) also show Lewis acidity in the presence of molecular oxygen. It is well known that super-oxide-like species, useful for catalytic aerobic oxidation reactions, are generated after the absorption of oxygen (Fig. 1B)⁸. At the same moment, the surface of gold near the absorption site becomes positively charged, resulting in Lewis acidity^{9–11}. Previous studies revealed that intermolecular hydroamination^{12,13} proceeded in the presence of the Au:PVP [PVP: poly(*N*-vinyl-2-pyrrolidone)] under aerobic conditions (Fig. 1C)^{14–16}. The terminal and/or internal alkenes were activated at the cationic site with the help of molecular oxygen to afford cyclic amines, commonly found in natural products and pharmaceuticals. This study investigated other stabilising supports, mainly polymer-based matrices, which combine high catalytic activity with ease of use.

Our former studies proposed that Au NPs stabilised by biomacromolecules, such as chitin and chitosan, showed superior catalytic activity rather than that of PVP in some cases^{17,18}. For example, Au NPs stabilised by chitin or chitosan were found suitable for homocoupling reaction of phenylboronic acids because of auxiliary functional groups, such as amine and amide¹⁹. The localised basic environment nearby the reaction site prevented the unfavoured oxidation pathway and therefore increased the chemoselectivity of this reaction. This example suggests that a functionalised polymer matrix can effectively control the response. Recently, we have developed a concise preparation method to fabricate fibrillated cellulose by chemical modification using citric acid (F-CAC)^{20,21}. In addition, we have developed a size-selective preparation method to afford Au NPs stabilised on F-CAC (Au:F-CAC). They were applied for aerobic oxidation of benzylic alcohols^{22,23}. Since the Au NP-catalysed hydroamination reaction proceeds under slightly acidic conditions ($\text{pH} = 4$), we considered that the F-CAC, bearing carboxylic acid moieties, is a suitable matrix to facilitate the hydroamination reaction. Additionally, the high tolerance against organic solvents and their recyclability renders the reaction practical. Herein, we report a matrix effect of F-CAC toward hydroamination reaction (Fig. 1D).

Results and discussions

Optimisation of reaction conditions. Our attempt commenced with an intramolecular hydroamination reaction of **1a** using Au:F-CAC (particle size of Au: 1.7 ± 0.2 nm, 1.68×10^{-3} wt%) prepared by the trans-deposition method^{22,24,25}. In the presence of Au:F-CAC (5 mol%), the reaction was performed in buffer/EtOH solution under the aerobic condition to afford pyrrolidine **2a** in quantitative yield without any side products, such as **3a** or **4a** (Table 1, entry 1, and Table S1). It should be noted that intermolecular addition of ammonia did not proceed because of its low nucleophilicity, and entropically favorable intramolecular reaction occurs much faster. When the reaction was carried out without an additional formic acid, which acts as a reducing agent,

¹Division of Applied Chemistry, Graduate School of Engineering, Osaka University, 2-1 Yamadaoka, Suita, Osaka 565-0871, Japan. ²Innovative Catalysis Science Division, Institute for Open and Transdisciplinary Research Initiatives (ICS-OTRI), Osaka University, 2-1 Yamadaoka, Suita, Osaka 565-0871, Japan. ✉email: hsakurai@chem.eng.osaka-u.ac.jp

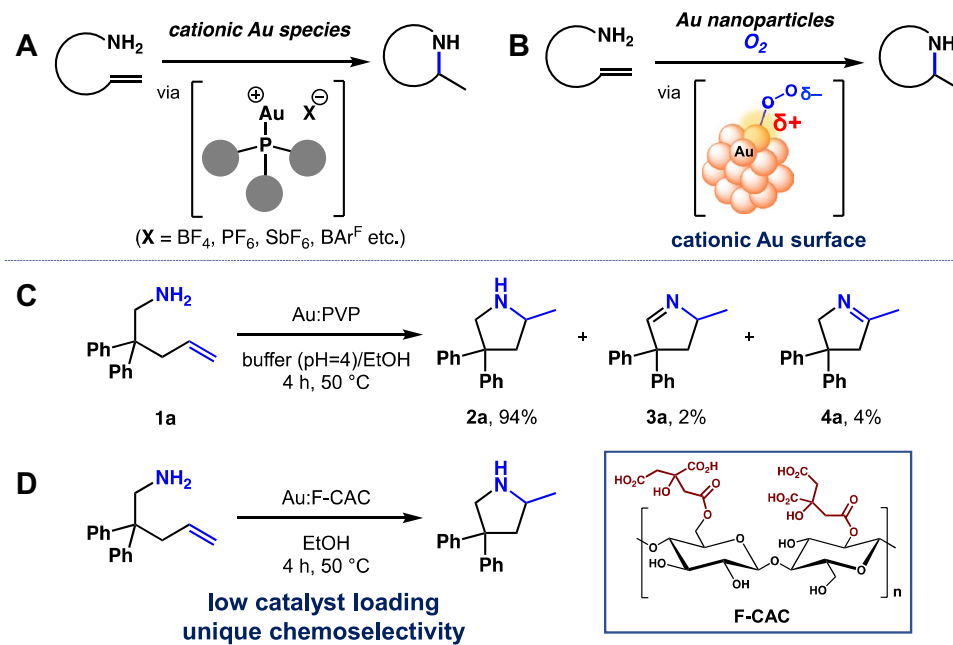


Figure 1. Cationic Au-catalysed intermolecular cycloamination reaction. **(A)** Homogeneous catalysis. **(B)** Heterogeneous catalysis. **(C)** Previous work using Au:PVP. **(D)** This work using Au:F-CAC. ArF: Tetrakis[3,5-bis(trifluoromethyl)phenyl].

Entry	Au NPs (mol%)	Additives (mol%)	Time (h)	Recovery of 1a (%) ^a	Yield of 2a (%) ^a	Leaching (%)
1	Au:F-CAC (5)	HCO ₂ H (1000) aq. NH ₃ (2000)	4	0	99	n.d.
2	Au:F-CAC (5)	aq. NH ₃ (500)	4	100	0	n.d.
3	Au:F-CAC (2)	HCO ₂ H (1000) aq. NH ₃ (2000)	10	0	99	45
4 ^b	Au:F-CAC (2)	HCO ₂ H (1000) aq. NH ₃ (2000)	4	0	99	25
5 ^b	Au:F-CAC (2)	HCO ₂ NH ₄ (500)	4	0	99	0
6 ^b	Au:F-CAC (0.5)	HCO ₂ NH ₄ (500)	4	0	99 (99) ^c	n.d.
7 ^b	Au:F-CAC (0.2)	HCO ₂ NH ₄ (500)	8	0	99 (99) ^c	n.d.
8 ^b	Au:F-CAC (0.5)	HCO ₂ NH ₄ (500)	2	13	85	n.d.
9 ^b	Au:PVP (0.5)	HCO ₂ NH ₄ (500)	2	47	45	n.d.
10 ^b	Au:PVP (0.2)	HCO ₂ NH ₄ (500)	8	52	46	n.d.
11 ^b	Au:PVP (0.2)	HCO ₂ NH ₄ (500)	24	43	55	n.d.

Table 1. Optimisation of reaction conditions. ^aDetermined by ¹H NMR analysis. ^bAbsolute EtOH was used as a solvent. ^cIsolated yield in parentheses.

the reaction did not proceed, indicating that the citric acid moiety in F-CAC does not work as a reducing agent (entry 2). Although a slight extension of the reaction time was required, the reaction took place with 2 mol% of Au:F-CAC without any loss of the yield of **2a** (entry 3). At this stage, we performed an inductively coupled plasma-atomic emission spectroscopy (ICP-AES) measurement of the Au:F-CAC after reaction to find severe leaching of gold from F-CAC (45% Au loss). As proposed in the previous work, the leaching of gold occurred when polar solvents, such as water, DMF, and DMSO, were used²². To reduce the amount of water in the solvent, we optimised the solvent system using 2 mol% of Au:F-CAC. The reaction did not proceed in toluene; however,

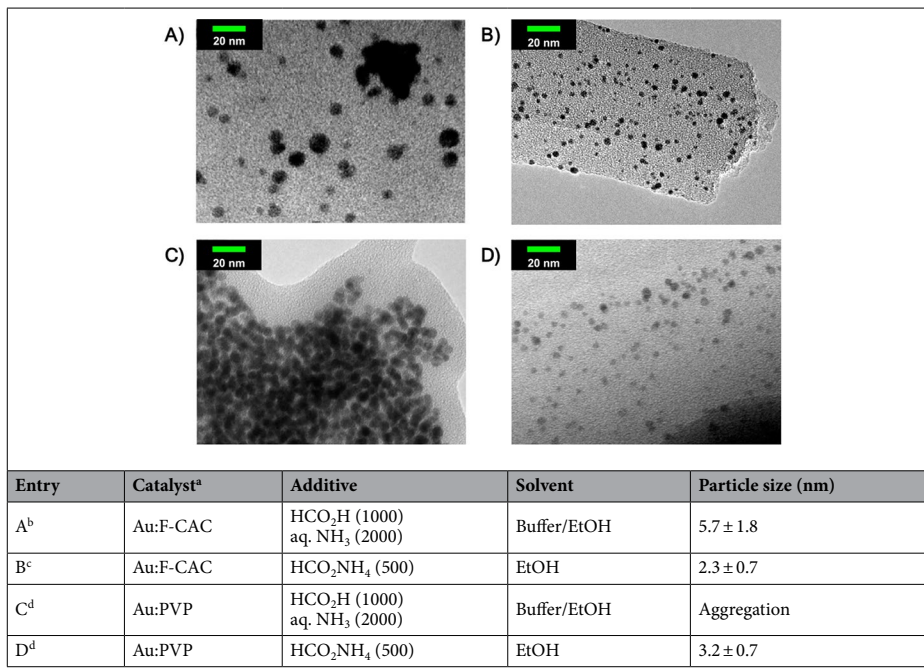


Table 2. TEM images and particle sizes of Au:F-CAC and Au:PVP after reaction. ^a2 mol% of Au NPs was used. ^bEntry 4 in Table 1. ^cEntry 5 in Table 1. ^dAu:PVP(K-30) (1.5 ± 0.2 nm) was used.

we found that the use of absolute EtOH showed a better result (25% Au loss) than the case of the buffer/EtOH system (entry 4). Finally, the use of ammonium formate (500 mol%), instead of liquid ammonium and formic acid, in EtOH completely suppresses the leaching of gold with retaining its high catalytic activity (entry 5). Given our previous theoretical studies²⁶, the use of excess amount of ammonium formate would accelerate the cleavage of Au–C bond to expel the cyclized product. Under the reaction conditions, the amount of gold could be reduced to 0.2 mol%, prolonging the reaction time by 8 h (entries 6 and 7). To compare their catalytic activities, we also performed the reaction using Au:PVP under the same conditions to find that Au:F-CAC showed a higher yield (85%) than Au:PVP (45%) at the point after 2 h (entries 8 and 9). The difference in catalytic activity was more pronounced when the amount of Au was compared at 0.2 mol% (entries 7 and 10), and the reaction did not complete even when the reaction was prolonged to 24 h in the case of Au:PVP (entry 11). These results suggested the high stability of Au NPs under the reaction conditions. Despite 0.2 mol% prolonging the reaction time of 8 h, the substrate scope is limited to **1a**. Thus, the reaction conditions of entry 6 were selected as an optimisation condition due to the requirement of an additional amount of gold in the substrates that have substituents at the alkene position (Fig. 3, *vide infra*).

The durability and reusability of Au:F-CAC. To gain insight into the catalytic activity of Au:F-CAC, Au NPs after the reaction were observed by transmission electron microscopy (TEM). As in our previous investigation, the severe aggregation of Au:PVP was observed under the aqueous conditions (Table 2, entry C)¹⁵. Meanwhile, the aggregation of Au NPs was suppressed to some extent in the case of Au:F-CAC (entry A). The use of solid ammonium formate in absolute EtOH was found to suppress the aggregation in both cases. However, the particle size of Au:F-CAC was much smaller than that of Au:PVP (entries B and D), leading to the high catalytic activity of the Au:F-CAC catalyst.

Next, the reusability test of Au:F-CAC catalyst was conducted to evaluate its durability (Fig. 2). After each reaction, the catalyst was filtered and washed with ethanol. After drying overnight, the spent catalyst was subjected to the next cycle. The hydroamination of **1a** proceeded almost quantitatively after 4 h in the 2nd cycle. Although a substantial decrease in the catalytic activity was observed after 3rd cycle, **2a** was still obtained in moderate yields (59–71%). TEM observations of the spent catalyst (after six cycles) showed slightly aggregated Au NPs (3.2 ± 0.2 nm), suggesting that the decrease of the catalytic activity would be ascribed to the decrease of the surface area of Au NPs.

The effect of the reaction atmosphere. The atmosphere of the reaction was investigated using 0.5 mol% Au:F-CAC. The yield of **2a** was almost unchanged between aerobic and oxygen atmospheres, indicating that the partial pressure of oxygen does not affect the reaction rate (Table 3, entries 1 and 2). This result suggested that the absorption of oxygen atoms does not include in the rate-determining step of the reaction. Indeed, we reported a theoretical investigation of the reaction mechanism of hydroamination reaction using the density functional theory (DFT) method²⁶, and concluded that the reductive elimination step would be the rate-determining step.

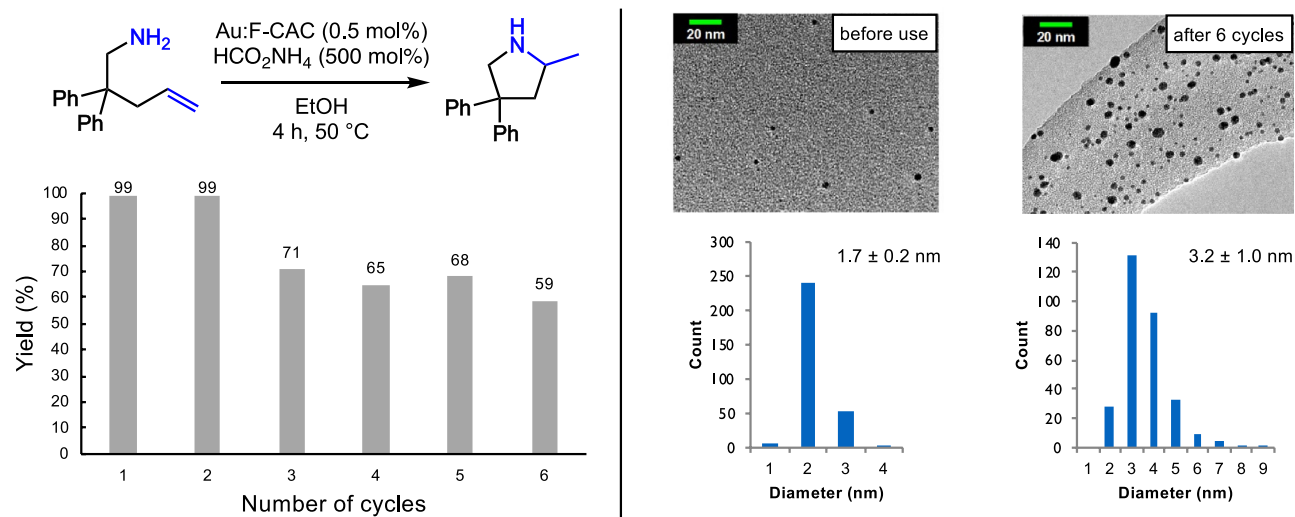
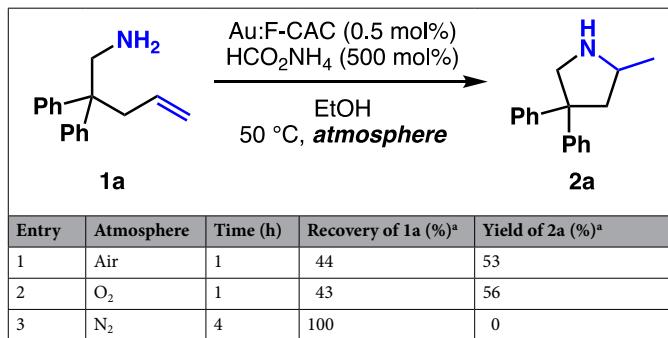


Figure 2. Reusability test of Au:F-CAC.

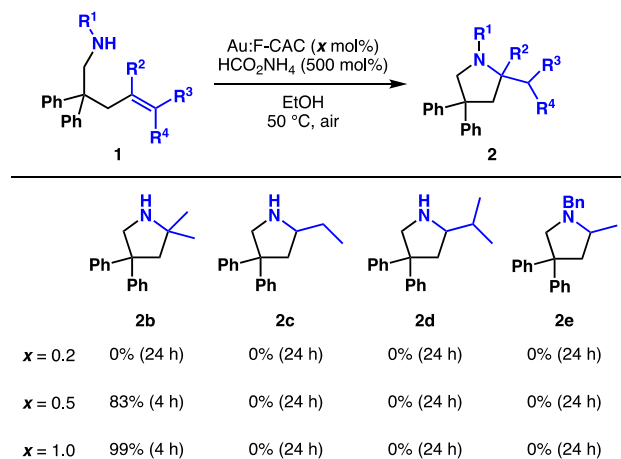
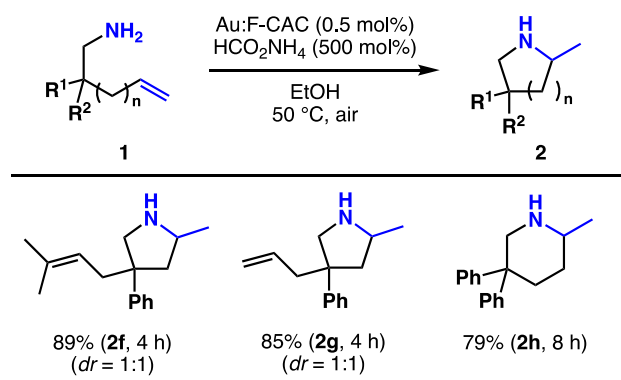
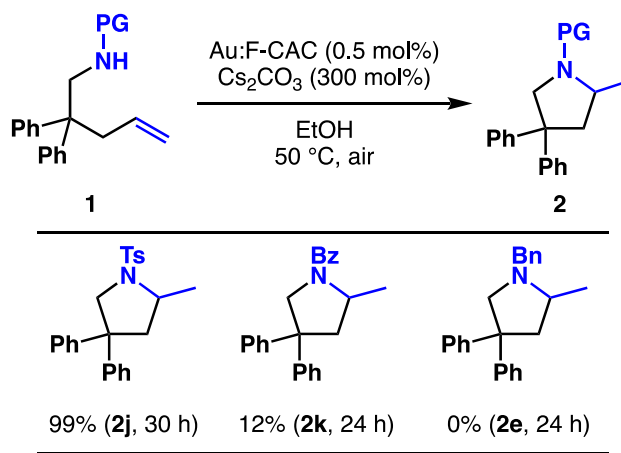
Table 3. Effect of the reaction atmosphere. ^aDetermined by ¹H NMR analysis.

Therefore, this experimental result is consistent with the theoretical calculations. As expected, the cyclisation did not proceed under a nitrogen atmosphere, indicating that oxygen is crucial for this reaction (entry 3).

Substrate scope. The substrates having different substituents and protecting groups were subjected to the reaction (Fig. 3). Although a primary amine having a β -methyl group did not participate in this reaction under an optimised reaction condition (Table 1, entry 7), the cyclisation proceeded with 0.5 mol% Au loading to afford pyrrolidine 2b in 83% yield. Moreover, 2b was obtained quantitatively when 1.0 mol% Au:F-CAC was used. Primary amines bearing crotyl (1c) and prenyl group (1d) did not participate in the reaction even when extending time or increasing the amount of catalyst, probably because of sterically hindered di- or tri-substituted alkene. Unlike in the case of cationic gold complexes, these reaction conditions are likely to be more sensitive to steric factors in the case of AuNPs, since there are multiple gold species adjacent to the cationic Au site activated by oxygen. Therefore, the reaction conditions were expected to allow chemoselective hydroamination of terminal alkenes. The use of benzyl-protected amine (1e) resulted in the decomposition of the starting material. This is probably due to the unstable nature of benzylamine to the oxidising ability of the AuNPs/O₂ condition.

The substrates having different substituents at the β -position of the amino group were investigated (Fig. 4). As expected from the result that the reaction conditions are sensitive to the steric hindrance of alkene moiety, the chemoselective cyclisation of an amine with biased olefins is an excellent example of this unique system. The cyclisation of an amine having both allyl and prenyl group (1f) was subjected to this reaction to find that the cyclisation occurred at the allyl site to give 2f (89%) with complete chemoselectivity (dr = 1:1). The reaction of an amine having a diallyl group (1g) also provides desired product 2g (85%) within 4 h. The reaction proceeded smoothly when the amine-bearing homoallyl group (1h) was used, affording piperazine 2h in 79%.

We then applied the reaction conditions to the amines having protecting groups, such as toluenesulfonyl (1j) and benzoyl (1k) groups; however, it was found that the cyclisation reaction did not occur. After several attempts, we found that caesium carbonate (Cs_2CO_3) was adequate for the intermolecular cyclisation reaction to increase the nucleophilicity of amides. Pyrrolidine 2j was obtained in quantitative yield when the sulfonimines 1j were treated with 0.5 mol% of Au:F-CAC and 300 mol% of Cs_2CO_3 under an aerobic atmosphere at 50 °C for

**Figure 3.** Scope of alkenes.**Figure 4.** The substrate scope of intramolecular cyclisation of primary amine. *dr* diastereomeric ratio.**Figure 5.** The substrate scope of protected amines.

30 h (Fig. 5). Although amide (1k) participated in this reaction, albeit in low yield (12%), the reaction did not proceed in the case of benzylamine 1e, even under the reaction conditions.

Conclusions

In summary, the Au:F-CAC catalyst shows high catalytic activity for the hydroamination reaction. The concentration of Au can be reduced up to 0.2 mol%. By focusing on the fact that this catalyst is substantially affected by the substitution pattern of alkene moiety, we achieved unprecedented chemoselective cyclisation, which has been

difficult to perform in conventional cationic Au-catalysed reactions, affording novel compounds. Further investigations, such as application for the synthesis of fine chemicals and reaction developments, are in due course.

Data availability

The main data are available in the main text or the Supplementary Information. All other data are available from the authors upon reasonable request.

Received: 3 October 2022; Accepted: 22 November 2022

Published online: 29 November 2022

References

1. Campeau, D., León Rayo, D. F., Mansour, A., Muratov, K. & Gagasz, F. Gold-catalyzed reactions of specially activated alkynes, alkenes, and alkynes. *Chem. Rev.* **121**, 8756–8867 (2021).
2. Gorin, D. J. & Toste, F. D. Relativistic effects in homogeneous gold catalysis. *Nature* **446**, 395–403 (2007).
3. Hashmi, A. S. K. Dual gold catalysis. *Acc. Chem. Res.* **47**, 864–876 (2014).
4. Müller, T. E., Hultsch, K. C., Yus, M., Foubelo, F. & Tada, M. Hydroamination: Direct addition of amines to alkenes and alkynes. *Chem. Rev.* **108**, 3795–3892 (2008).
5. Müller, T. E. & Beller, M. Metal-initiated amination of alkenes and alkynes. *Chem. Rev.* **98**, 675–704 (1998).
6. Hashmi, A. S. K. Gold-catalyzed organic reactions. *Chem. Rev.* **107**, 3180–3211 (2007).
7. Dorel, R. & Echavarren, A. M. Gold(I)-catalyzed activation of alkynes for the construction of molecular complexity. *Chem. Rev.* **115**, 9028–9072 (2015).
8. Bistoni, G., Belanzoni, P., Belpassi, L. & Tarantelli, F. π activation of alkynes in homogeneous and heterogeneous gold catalysis. *J. Phys. Chem. A* **120**, 5239–5247 (2016).
9. Kamiya, I., Tsunoyama, H., Tsukuda, T. & Sakurai, H. Lewis acid character of zero-valent gold nanoclusters under aerobic conditions: Intramolecular hydroalkoxylation of alkenes. *Chem. Lett.* **36**, 646–647 (2007).
10. Tsunoyama, H., Ichikuni, N., Sakurai, H. & Tsukuda, T. Effect of electronic structures of Au clusters stabilized by poly(*N*-vinyl-2-pyrrolidone) on aerobic oxidation catalysis. *J. Am. Chem. Soc.* **131**, 7086–7093 (2009).
11. M Palashuddin, S. K., Jana, C. K. & Chattopadhyay, A. A gold-carbon nanoparticle composite as an efficient catalyst for homo-coupling reaction. *Chem. Commun.* **49**, 8235–8237 (2013).
12. Huang, J., Arndt, M., Gooßen, K., Heydt, H. & Gooßen, L. J. Late transition metal-catalyzed hydroamination and hydroamidation. *Chem. Rev.* **115**, 2596–2697 (2015).
13. Sengupta, M., Das, S., Islam, S. M. & Bordoloi, A. Heterogeneously catalysed hydroamination. *ChemCatChem* **13**, 1089–1104 (2021).
14. Kitahara, H., Kamiya, I. & Sakurai, H. Intramolecular addition of toluenesulfonamide to unactivated alkenes catalyzed by gold nanoclusters under aerobic conditions. *Chem. Lett.* **38**, 908–909 (2009).
15. Kitahara, H. & Sakurai, H. Gold nanoclusters as a catalyst for intramolecular addition of primary amines to unactivated alkenes under aerobic conditions. *Chem. Lett.* **39**, 46–48 (2009).
16. Kitahara, H. & Sakurai, H. Addition-versus-oxygenative cleavage: Two contradictory reactivities in the reaction of *N*-Benzyl-4-pentenylamine catalyzed by colloidal nanogold under aerobic conditions. *Chem. Lett.* **41**, 1328–1330 (2012).
17. Jiménez-Gómez, C. P. & Cecilia, J. A. Chitosan: A natural biopolymer with a wide and varied range of applications. *Molecules* **25**, 3981 (2020).
18. Shaghaleh, H., Xu, X. & Wang, S. Current progress in production of biopolymeric materials based on cellulose, cellulose nanofibers, and cellulose derivatives. *RSC Adv.* **8**, 825–842 (2018).
19. Dhitai, R. N., Murugadoss, A. & Sakurai, H. Dual roles of polyhydroxy matrices in the homocoupling of arylboronic acids catalyzed by gold nanoclusters under acidic conditions. *Chem. Asian. J.* **7**, 55–59 (2012).
20. Cui, X., Honda, T., Asoh, T.-A. & Uyama, H. Cellulose modified by citric acid reinforced polypropylene resin as fillers. *Carbohydr. Polym.* **230**, 115662 (2020).
21. Sinawang, G. *et al.* Citric acid-modified cellulose-based tough and self-healable composite formed by two kinds of noncovalent bonding. *ACS Appl. Polym. Mater.* **2**, 2274–2283 (2020).
22. Chutimasakul, T. *et al.* Size-controlled preparation of gold nanoparticles deposited on surface-fibrillated cellulose obtained by citric acid modification. *ACS Omega* **5**, 33206–33213 (2020).
23. Haesuwannakij, S. *et al.* The impact of the polymer chain length on the catalytic activity of poly(*N*-vinyl-2-pyrrolidone)-supported gold nanoclusters. *Sci. Rep.* **7**, 9579 (2017).
24. Tsunoyama, H., Sakurai, H., Negishi, Y. & Tsukuda, T. Size-specific catalytic activity of polymer-stabilized gold nanoclusters for aerobic alcohol oxidation in water. *J. Am. Chem. Soc.* **127**, 9374–9375 (2005).
25. Tsunoyama, H., Sakurai, H. & Tsukuda, T. Size effect on the catalysis of gold clusters dispersed in water for aerobic oxidation of alcohol. *Chem. Phys. Lett.* **429**, 528–532 (2006).
26. Bobuatong, K., Sakurai, H. & Ehara, M. Intramolecular hydroamination by a primary amine of an unactivated alkene on gold nanoclusters: A DFT study. *ChemCatChem* **9**, 4490–4500 (2017).

Acknowledgements

We thank Prof. Hiroshi Uyama and Taka-aki Asoh (Osaka University) for their support in preparing F-CAC. This work was supported by Grant-in-Aid for Scientific Research on the Japan Society for the Promotion of Science (JSPS) KAKENHI (JP20K15279 and 22K05095, YU; JP19K22187, HS); the JST-Mirai Program (JPMJMI18E3). BS acknowledges JSPS for the scholarship.

Author contributions

H.S. directed the project and constructed the scientific plan. Y.U. managed the project and wrote the manuscript mainly. B.S. operated the experiments, wrote the draft of the manuscript, and prepared the supporting information. All authors reviewed the manuscript.

Competing interests

The authors declare no competing interests.

Additional information

Supplementary Information The online version contains supplementary material available at <https://doi.org/10.1038/s41598-022-24955-3>.

Correspondence and requests for materials should be addressed to H.S.

Reprints and permissions information is available at www.nature.com/reprints.

Publisher's note Springer Nature remains neutral with regard to jurisdictional claims in published maps and institutional affiliations.



Open Access This article is licensed under a Creative Commons Attribution 4.0 International License, which permits use, sharing, adaptation, distribution and reproduction in any medium or format, as long as you give appropriate credit to the original author(s) and the source, provide a link to the Creative Commons licence, and indicate if changes were made. The images or other third party material in this article are included in the article's Creative Commons licence, unless indicated otherwise in a credit line to the material. If material is not included in the article's Creative Commons licence and your intended use is not permitted by statutory regulation or exceeds the permitted use, you will need to obtain permission directly from the copyright holder. To view a copy of this licence, visit <http://creativecommons.org/licenses/by/4.0/>.

© The Author(s) 2022